Electron acceleration to energies beyond GeV by a relativistic ion beam instability

M. E. Dieckmann,* B. Eliasson,† and P. K. Shukla‡
Institut für Theoretische Physik IV, Ruhr-Universität Bochum, D-44780 Bochum, Germany
(Received 12 January 2004; published 10 September 2004)

Synchrotron emission suggests the presence of TeV electrons at various astrophysical objects. We propose a mechanism for the acceleration of electrons to ultrahigh energies (UHE) by intense electrostatic waves (ESWs). The latter are driven by dense proton beams that move at relativistic speeds relative to a background plasma and the electrons are accelerated by their nonlinear interaction with the ESWs. We follow the evolution of the wave instability by means of particle-in-cell (PIC) simulations. After the instability has saturated, we obtain spatially confined electron voids in which secondary instabilities develop due to resonant interactions between the beams and the background protons, generating intense ESWs which accelerate electrons to ultrarelativistic speeds within times of a few hundred inverse plasma frequencies.

DOI: 10.1103/PhysRevE.70.036401 PACS number(s): 96.50.Qx, 52.35.Sb, 96.50.Pw, 98.70.Rz

The emission of radio synchrotron emission by galactic sources [1] and by extragalactic sources [2–6] suggests the presence of electrons with ultrahigh energies (UHE). Electron Fermi acceleration across shocks is believed to be a major acceleration mechanism [1,2]. Plasma wakefield acceleration [7], shock surfing acceleration [8,9], and electron acceleration by electrostatic wave turbulence have also been invoked [10]. In the latter case, the electrons are accelerated by their interaction with electrostatic waves (ESWs) [10,11]. The ESWs are excited by ion beams streaming at high speeds relative to the background plasma which are found in front of plasma shocks due to the leaking of hot downstream ions into the foreshock, and because upstream ions are reflected by the shock and thereafter move through the foreshock region at a speed that exceeds that of the shock [12].

Previous simulations [13] have shown that an instability develops due to resonant interactions between the electrons and the ion beam. The ESWs saturate by trapping electrons and even in an unmagnetized plasma a substantial number of electrons is accelerated to speeds that significantly exceed the phase speed of the ESWs [13,14]. However, the instability transfers only a small fraction of the ion beam energy to the electrons. The intense releases of UHE electrons observed at radio synchrotron sources would thus require unrealistically high ion beam energies.

In this work, we present a more efficient mechanism for generating ultraintense electrostatic fields that are required for accelerating electrons to UHE. Our proposed mechanism involves the complete thermalization of the ion population and an equipartition of the plasma kinetic energy between the protons and electrons. Specifically, we consider collective interactions between highly relativistic proton beams and the background plasma and show, by means of particle-in-cell (PIC) simulations, the possibility of a fastest growing beam-plasma instability which saturates by trapping electrons. The electrons form a plateau in momentum space [15]. The electrons initially react quasineutrally to the electric field originating from charge density fluctuations in the proton beam. The relativistic Lorentz contraction of the proton beam and the chosen initial value for the beam density, however, imply that the beam has a considerably larger charge density than the electrons, and we find that already a weak charge density modulation on the beam can locally deplete the electron distribution. Therefore, the condition in Ref. [16] stating that two ion beams can interact directly only if their relative speed is low compared to the thermal speed of the electrons is removed, and the system becomes unstable which we confirm here. A secondary instability involving the interaction between a proton beam, the background protons and electrons generates intense ESWs which rapidly accelerate electrons to ultrarelativistic speeds. We measure a high energy tail of the electrons that is a power law up to a Lorentz factor of $\gamma > 4 \times 10^4$, and by taking into account the much larger number of electrons in a physical plasma than in our simulation it may reach well into the TeV regime.

Our results are obtained by means of a fully relativistic and electromagnetic PIC code [17]. The simulations model one spatial and three velocity components. The spatial boundary conditions of the simulation are periodic. The plasma consists of four particle species, labeled by the index j which takes the value *el* for the background electrons, *bp* for the background protons, and the two counter-propagating proton beams are represented by $b1$ and $b2$, respectively. The species *el* and *bp* represent the upstream plasma in front of the shock. The first beam represents the protons that have just been reflected by the shock. This beam rotates in the upstream magnetic field and it returns to the shock as the second beam. This model is in agreement with the simple model for a foreshock that we have used previously [13–15].

We define the initial thermal speeds of each plasma species by $v_{th,j} = (k_B T_j / m_j)^{1/2}$, where T_j and m_j are the temperature and mass of the jth species, respectively, and k_B is the Boltzmann constant. The plasma frequency of the jth species is defined in the rest frame of the electrons as $\omega_{p,j} = (n_j e^2 / \epsilon_0 m_j)^{1/2}$, where n_j is the particle number density of species j, e is the magnitude of the electron charge, and ϵ_0 is

*Electronic address: mardi@itn.liu.se; on leave from ITN, Linköpings University, 60174 Norrköping, Sweden.
†Electronic address: bengt@tp4.rub.de
‡Electronic mail: ps@tp4.rub.de

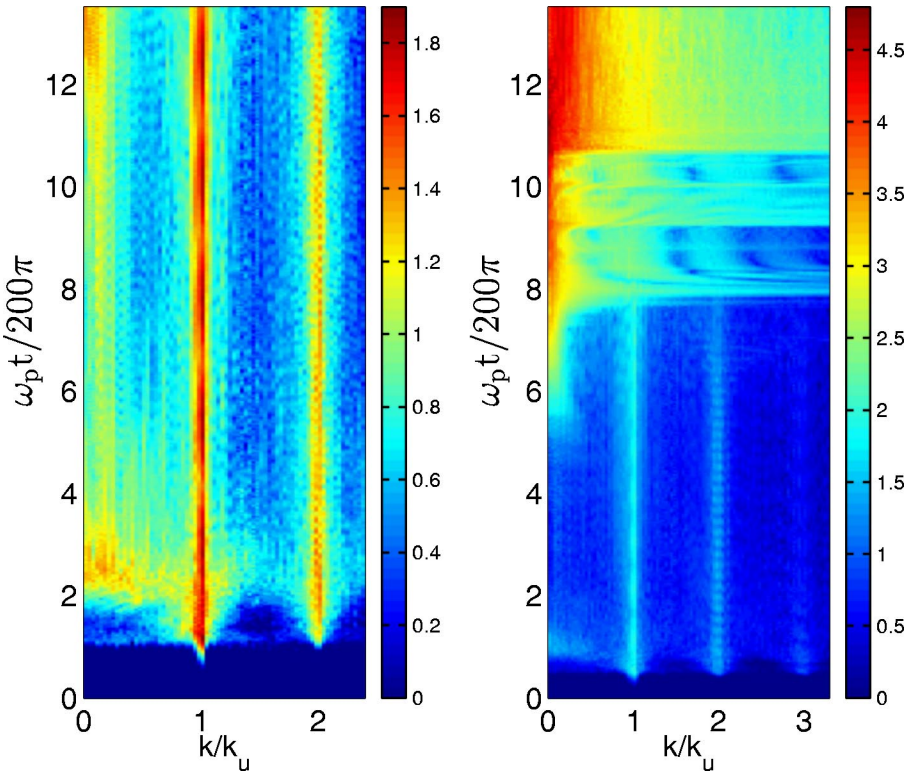

FIG. 1. The power spectrum $A(n,t)$ for the simulation with the beam density $n_b=n_{el}$ (left plot) and the simulation with $n_b=7.1n_{el}$ (right plot). In both simulations, an ESW initially grows at the wave number k_u. This ESW is sufficiently strong to produce a harmonic at $k=2k_u$. In the left plot, the ESW stabilizes after its initial saturation. In the right plot we find growing low-k waves at $t\approx 600\times 2\pi/\omega_p$. At $t\approx 800\times 2\pi/\omega_p$, the spectrum is increasingly bursty and the waves spread over a large k interval. After $t\approx 1050\times 2\pi/\omega_p$, the spectrum exhibits a continuous power law.

the electric vacuum permittivity. We set $v_{th,j}$ in the rest frame of the respective plasma species to $v_{th,el}=1.06\times 10^{-2}c$ and $v_{th,bp}=v_{th,b1}=v_{th,b2}=7.8\times 10^{-4}c$.

The electron density n_{el} in our simulation gives the electron plasma frequency $\omega_p=10^5\times 2\pi s^{-1}$. We will omit the index *el* for the electron plasma frequency. The density of the background protons is $n_{bp}=n_{el}$ and those of the two proton beams are $n_{b1}=n_{b2}\equiv n_b$ in their respective rest frame. We will consider the two cases $n_b=n_{el}$ and $n_b=7.1n_{el}$. The electrons and the background proton species have the mean speeds $\hat{v}_{el}=0$ and $\hat{v}_{bp}=0$. The two proton beams move at the mean speeds $\hat{v}_{b1}=-\hat{v}_{b2}=0.99c$. We obtain current neutrality in our simulation box which is necessary, since otherwise our periodic boundary conditions would yield (unphysical) waves growing with the wave number $k=0$. The excess positive charge of the protons is compensated by the simulation by introducing an immobile negative charge. This could, for example, be high-Z negative ions or negatively charged dust grains.

Initially, the electrons interact with the proton beams. We can separate the dispersion relation into two component equations, each involving one proton beam and the electrons. The cold plasma dispersion relation for the ESWs in the presence of the beam $b1$ with $\hat{v}_{b1}>0$ and the electrons is

$$1-\frac{\omega_p^2}{\omega^2}-\frac{\omega_{p,b1}^2\gamma(\hat{v}_{b1})^{-3}}{(\omega-k\hat{v}_{b1})^2}=0, \tag{1}$$

which yields the maximum growth rate for the ESWs as

$$\Gamma=\gamma^{-1}\left(3\frac{\sqrt{3}}{16}\omega_{p,b1}^2\omega_p\right)^{1/3}. \tag{2}$$

The wavelength of the most unstable ESW is $\lambda_u\approx 2\pi v_{b1}/\omega_p$ and $k_u=2\pi/\lambda_u$. Our simulation box has the length $L=120\lambda_u$ in the x direction. Each proton species is represented by 1 776 000 computational particles and the electrons by 2 557 440 computational particles.

We calculate the logarithmic amplitude spectra of the resulting ESWs by means of the expression

$$A(n,t)=\log_{10}\left|N^{-1}\sum_{l=1}^{N}E(l,t)\exp(-i\Delta k\Delta x n l)\right|, \tag{3}$$

where $E(l,t)$ is the electrostatic field in physical units (V/m) in the x direction, which is measured at the position $l\Delta x$ and time t. We use $N=5920$ grid cells. The minimum nonzero wave number is $\Delta k=2\pi(N\Delta x)^{-1}$, and the physical wave numbers are defined as $k=n\Delta k$. We show $A(n,t)$ for the simulations in Fig. 1

Figure 1 reveals that the ESW with the wave number k_u in our simulation with $n_b=7.1n_{el}$ initially saturates. After $t\approx 500\times 2\pi/\omega_p$, a second wave grows at low k which we could not find for significantly lower beam densities. This wave grows until it saturates at $t\approx 800\times 2\pi/\omega_p$. Until $t\approx 10^3\times 2\pi/\omega_p$, most of its wave power is concentrated at $k<k_u$, but we find time-dependent high-k spikes extending above k_u. This spectrum changes into a time-stationary spectrum power law at $t\approx 1050\times 2\pi/\omega_p$, with its power scaling like $A(k)A(k)^*\approx C_0(k/k_u)^{-3.4}$.

To understand the mechanism behind these low-k oscillations we show the electrostatic field in our simulation at four different times in Fig. 2. The two spikes visible in the upper right panel (at $t=600\times 2\pi/\omega_p$) in Fig. 2 are a key element for the further time evolution of our system, since they breach the equilibrium that has been established between the ESWs and the electrons. We show the peak electric field amplitude of the stronger of the two spikes in Fig. 3 as a

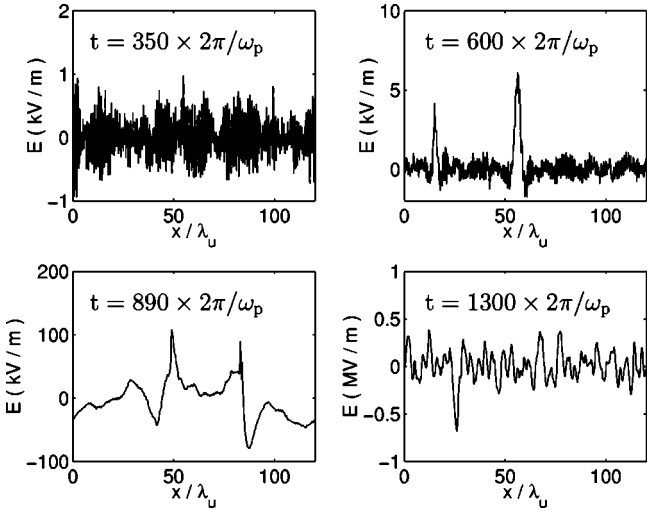

FIG. 2. The electric field E at time $t=350\times 2\pi/\omega_p$ (upper left panel), $t=600\times 2\pi/\omega_p$ (upper right panel), $t=890\times 2\pi/\omega_p$ (lower left panel), and $t=1300\times 2\pi/\omega_p$ (lower right panel). Two spikes which move with $v\approx 0.9c$ are visible at $t=600\times 2\pi/\omega_p$. These spikes evolve initially into the low-k oscillations at $t=890\times 2\pi/\omega_p$ and thereafter into the extremely strong fluctuations at all spatial scales at $t=1300\times 2\pi/\omega_p$.

function of time. We find that the amplitude initially grows exponentially, $\sim\exp(\Gamma t)$, with the growth rate $\Gamma\approx 2\times 10^{-3}\omega_p$. In Fig. 4, we display the charge distribution of the beam moving with $\hat{v}_{b1}$ and the distribution of the electrons with $v_x>0$ at the time $t=600\times 2\pi/\omega_p$. We find modulations with a similar amplitude in the charge density of the proton beam with $v_b=0.99c$ and of the electrons with positive speeds at the locations where we have found the spikes in Fig. 2. The charge density oscillations on the proton beam account for only 2% of the total beam density. The electrons are, however, depleted in this interval. The electrons with

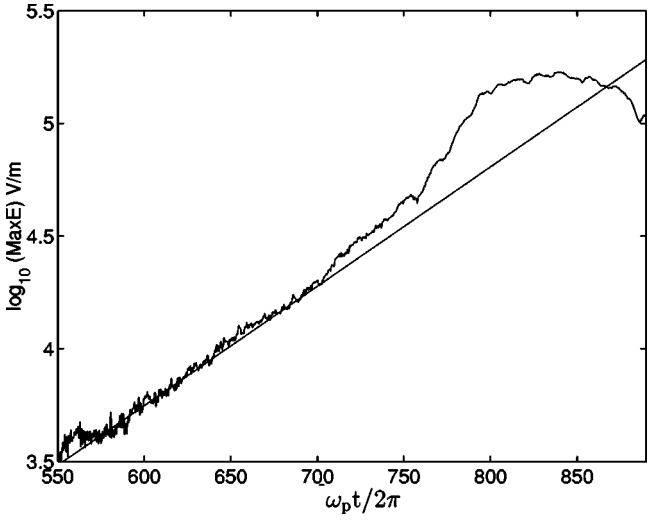

FIG. 3. The base-10 logarithm of the evolving maximum electric field of the largest spike in our simulation. Between the times $t=550\times 2\pi/\omega_p$ and $t=700\times 2\pi/\omega_p$ the wave amplitude grows exponentially. The increased growth after $t=700\times 2\pi/\omega_p$ is linked to the triggering of oscillations with a large spatial extent.

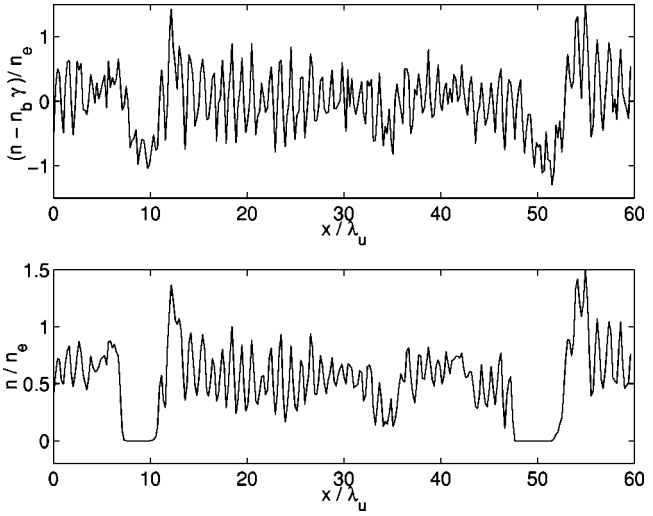

FIG. 4. The charge density fluctuations of the proton beam with $v_b=0.99c$ normalized to the electron density (upper plot), and the charge density distribution of the electrons with $v_x>0$ normalized to the total electron charge density (lower plot), at $t=600\times 2\pi/\omega_p$. Both plots show the same spatial interval of the simulation box. We observe that the depletions of the charge density in the proton beam at $x/\lambda_u\approx 8$ and $x/\lambda_u\approx 50$ are associated with intervals in which no electrons with $v_x>0$ are present.

$v_x<0$ show only a weak modulation and neither the bulk protons nor the beam with $v_b=-0.99c$ show visible charge density modulations, and we have thus not shown these here.

The charge density depletions move at the speed $v_x\approx 0.9c$ and they are thus not stationary in the frame of reference of the beam moving with v_b, they must thus be attributed to a wave. Since no electrons with positive speed can be found at the location of the spikes, the plasma in the half-space with $v_x>0$ consists only of the almost unperturbed proton beam with $v_b=0.99c$ and the bulk protons. Since the electric field in these electron density depletions grows against the thermal pressure of the surrounding electrons, it is likely to be a nonlinear wave. Within the electron void we may, however, approximate the plasma by a cold proton beam $b1$ and by the cold proton species bp, since their thermal spread at $t=500\times 2\pi/\omega_p$ is less than 1% of $\hat{v}_{b1}$. The dispersion properties of our plasma is then governed by

$$F(k,\omega)=1-\frac{\omega_{p,bp}^2}{\omega^2}-\frac{\omega_{p,b1}^2\gamma(v_{b1})^{-3}}{(\omega-k\hat{v}_{b1})^2}=0, \tag{4}$$

which we solve numerically for our plasma parameters to give the maximum growth rate $\Gamma\approx 4\times 10^{-3}\omega_p$ at the wave number $k_{u2}\approx 3\Delta k$. At this wave number we also obtain the phase speed $\omega_{u2}/k_{u2}\approx 0.87c$, which is approximately the same as the speed of the spikes. The ESWs are unstable up to a peak wave number $\approx 4\Delta k$. We note that the maximum growth rate corresponds exactly to the fastest growth rate observed in Fig. 3 for the time $t=750-800\times 2\pi/\omega_p$. In our simulation we find, due to the localization of the wave packet, a significant exponential growth up to a wave number $\approx 10\Delta k$ which exceeds the band of unstable k values. The wave packet thus leaks power to stable wave numbers which

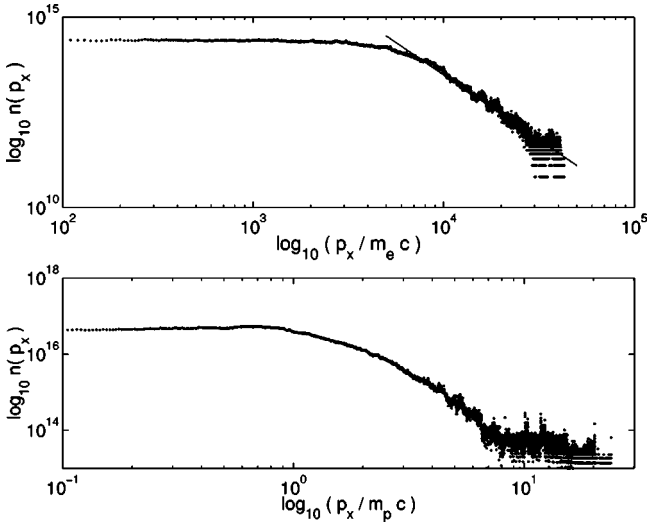

FIG. 5. The electron momentum space density (upper plot) and the momentum space density summed over all proton species (lower plot), at time $t=1300\times 2\pi/\omega_p$. Both distributions are given in terms of physical particles, i.e., we have multiplied the number of computational particles by a factor that expresses the ratio between simulation particle numbers and true particle numbers. The electrons have a flat distribution up to $p_x/m_ec\approx 10^3$. Above this momentum, the electron distribution has a spectrum that is well approximated by a power law, viz. $P(p_x)=C_1(p_x/m_ec)^{-3.4}$, which is the line we have overplotted. The lower plot shows that the protons have been fully thermalized.

may explain the measured reduced growth rate $\Gamma\approx 2\times 10^{-3}$ for the time $t<750\times 2\pi/\omega_p$, as seen in Fig. 3.

We observe that the power spectrum of the electric field eventually develops into a power law distribution with extremely strong electric field oscillations, which can be seen in the right plot in Fig. 1 and in the lower right plot in Fig. 2. We anticipate extremely hot electrons and protons at this time. In Fig. 5, we present the distribution of the particle momenta we obtain at the end of the simulation. Here, the particles have been accelerated by both the initial instability between the proton beam and the electrons and the second instability between the protons. We find that at the simulation end the plasma is fully thermalized, i.e., no further instability can trigger the ESWs along the x direction. We also find that both distributions are similar except for a scaling factor m_p/m_e on the Lorentz factors, i.e., both species have equal shares of the total kinetic energy. The power law of the electron momentum distribution has the same spectral slope as the electric field spectral density in Fig. 1 after $t\approx 1050\times 2\pi/\omega_p$ and it does not break up to the peak momentum $p_x/m_ec\approx 4.5\times 10^3$. It is limited only by the statistical representation of the simulation plasma. Extrapolating the power law to a momentum density that represents a single electron in our simulation box will give a peak momentum of the electron distribution of $p_x/(m_ec)\approx 10^8$ or an energy of around 50 TeV. For our initial conditions we have obtained a total acceleration time of $T_{\max}\approx 10^{-2}$ s $\approx 10^3\times 2\pi/\omega_p$, i.e., we have a very efficient wave accelerator.

To summarize, we have presented computer simulations of a sequence of two plasma instabilities that produces ESWs, which can rapidly accelerate electrons to UHE energies that may work if relativistic ion beams are present. Relativistic ion beams have been suggested to exist in astrophysical environments, such as, e.g., at blazars and at pulsars [4–6], as well as at quasiperpendicular shocks in the interstellar medium [8,9]. Our beam Lorentz factor of 7.1 is particularly interesting in the context of internal shocks at gamma ray bursts and at the relativistic jets of active galactic nuclei since there the plasma shocks and thus the shock reflected ions should have a similar Lorentz factor.

Our simulations show that a primary instability develops due to resonant interactions between the relativistic proton beams and the background electrons, and after its saturation the plasma is unstable to a secondary instability which develops due to resonant interactions between the relativistic proton beams and the background protons. A key element has been that the Lorentz contraction of the proton beams implies that even small charge density fluctuations on the beams depletes electrons, allowing for the development of an instability between the proton species. The instability is facilitated by the presence of high-Z negative ions of large mass or negatively charged dust, since it cannot rapidly react to charge fluctuations of the beam. Our simulations have also shown the appearance of extremely strong ESWs which thermalize all plasma species and produce a power law distribution for both the protons and electrons where the maximum speed scales like the mass ratio between the protons and electrons. The rapid relaxation of the shock-reflected beam implies that it thermalizes before it has been rotated by the upstream magnetic field to return to the shock. Our symmetric setup for the beams is thus not completely realistic, however, we emphasize that our conclusions do not depend on the presence of two symmetric beams. A single relativistic beam in the system gives rise to both the initial instability and the charge density fluctuations that lead to the second instability.

This work has been supported by the Swedish National Supercomputer Centre (NSC), by Linköpings University and by the European Community through the Contract No. HPRN-CT-2001-00314.

[1] S. R. Reynolds, Space Sci. Rev. **99**, 177 (2001).
[2] T. Piran, Phys. Rep. **314**, 575 (1999).
[3] F. A. Aharonian *et al.*, Phys. Rev. D **66**, 023005 (2002).
[4] W. Bednarek *et al.*, Astron. Astrophys. **307**, L17 (1996).
[5] W. Bednarek, Astrophys. J. **402**, L29 (1993).
[6] J. H. Beall and W. Bednarek, Astrophys. J. **510**, 188 (1999).
[7] P. Chen, T. Tajima, and Y. Takahashi, Phys. Rev. Lett. **89**, 161101 (2002).

[8] D. Ucer and V. D. Shapiro, Phys. Rev. Lett. **87**, 075001 (2001); E. L. Lever *et al.*, Geophys. Res. Lett. **28**, 1367 (2001).
[9] V. D. Shapiro and D. Ucer, Planet. Space Sci. **51**, 665 (2003); V. D. Shapiro *et al.*, J. Geophys. Res., [Space Phys.] **106**, 25023 (2001).
[10] R. Schlickeiser, Astron. Astrophys. **410**, 397 (2003).
[11] R. A. Treumann and T. Terasawa, Space Sci. Rev. **99**, 135 (2001).
[12] B. Lembege *et al.*, Space Sci. Rev. **110**, 161 (2004).
[13] M. E. Dieckmann *et al.*, Phys. Plasmas **7**, 5171 (2000).
[14] M. E. Dieckmann *et al.*, Phys. Rev. Lett. **92**, 065006 (2004).
[15] M. E. Dieckmann *et al.*, Phys. Plasmas **11**, 1394 (2004).
[16] R. A. Treumann and W. Baumjohann, *Advanced Space Plasma Physics* (Imperial College, London, 1997), p. 27.
[17] J. W. Eastwood, Comput. Phys. Commun. **64**, 252 (1991).